Acta Pharmaceutica Sinica B 2023;13(6):2701−2714

Chinese Pharmaceutical Association
Institute of Materia Medica, Chinese Academy of Medical Sciences

Acta Pharmaceutica Sinica B

www.elsevier.com/locate/apsb
www.sciencedirect.com

ORIGINAL ARTICLE

Corynoxine B targets at HMGB1/2 to enhance autophagy for α-synuclein clearance in fly and rodent models of Parkinson's disease

Qi Zhu[a,†], Juxian Song[b,c,†], Jia-Yue Chen[a,†], Zhenwei Yuan[c], Liangfeng Liu[c,d,e], Li-Ming Xie[a], Qiwen Liao[f], Richard D. Ye[f], Xiu Chen[a], Yepiao Yan[a], Jieqiong Tan[g], Chris Soon Heng Tan[h], Min Li[c,*], Jia-Hong Lu[a,*]

[a]*State Key Laboratory of Quality Research in Chinese Medicine, Institute of Chinese Medical Sciences, University of Macau, Macao 999078, China*
[b]*Medical College of Acupuncture-Moxibustion and Rehabilitation, Guangzhou University of Chinese Medicine, Guangzhou 510006, China*
[c]*Mr. and Mrs. Ko Chi Ming Centre for Parkinson's Disease Research, School of Chinese Medicine, Hong Kong Baptist University, HongKong 999077, China*
[d]*Guangdong Corporate Key Laboratory of High-end Liquid Medicine R&D, Industrialization, Shaoguan 512028, China*
[e]*Limin Pharmaceutical Factory, Livzon Pharmaceutical Group Inc., Shaoguan 512028, China*
[f]*Kobilka Institute of Innovative Drug Discovery, School of Medicine, the Chinese University of Hong Kong, Shenzhen 518172, China*
[g]*Center for Medical Genetics, Life Science School, Central South University, Changsha 410031, China*
[h]*Department of Chemistry, College of Science, Southern University of Science and Technology, Shenzhen 518055, China*

Received 14 October 2022; received in revised form 12 February 2023; accepted 28 February 2023

KEY WORDS

Corynoxine B;
Parkinson's disease;
Neurodegenerative

Abstract Parkinson's disease (PD) is the most common neurodegenerative movement disease. It is featured by abnormal alpha-synuclein (α-syn) aggregation in dopaminergic neurons in the substantia nigra. Macroautophagy (autophagy) is an evolutionarily conserved cellular process for degradation of cellular contents, including protein aggregates, to maintain cellular homeostasis. Corynoxine B

*Corresponding authors.
E-mail addresses: limin@hkbu.edu.hk (Min Li), jiahonglu@um.edu.mo (Jia-Hong Lu).
[†]These authors made equal contributions to this work.
Peer review under the responsibility of Chinese Pharmaceutical Association and Institute of Materia Medica, Chinese Academy of Medical Sciences.

https://doi.org/10.1016/j.apsb.2023.03.011

disease;
α-Synuclein;
Autophagy;
PI3KC3;
HMGB1;
HMGB2

(Cory B), a natural alkaloid isolated from *Uncaria rhynchophylla* (Miq.) Jacks., has been reported to promote the clearance of α-syn in cell models by inducing autophagy. However, the molecular mechanism by which Cory B induces autophagy is not known, and the α-syn-lowering activity of Cory B has not been verified in animal models. Here, we report that Cory B enhanced the activity of Beclin 1/VPS34 complex and increased autophagy by promoting the interaction between Beclin 1 and HMGB1/2. Depletion of HMGB1/2 impaired Cory B-induced autophagy. We showed for the first time that, similar to HMGB1, HMGB2 is also required for autophagy and depletion of HMGB2 decreased autophagy levels and phosphatidylinositol 3-kinase III activity both under basal and stimulated conditions. By applying cellular thermal shift assay, surface plasmon resonance, and molecular docking, we confirmed that Cory B directly binds to HMGB1/2 near the C106 site. Furthermore, *in vivo* studies with a wild-type α-syn transgenic drosophila model of PD and an A53T α-syn transgenic mouse model of PD, Cory B enhanced autophagy, promoted α-syn clearance and improved behavioral abnormalities. Taken together, the results of this study reveal that Cory B enhances phosphatidylinositol 3-kinase III activity/autophagy by binding to HMGB1/2 and that this enhancement is neuroprotective against PD.

1. Introduction

Parkinson's disease (PD) is the second most common neurodegenerative disorder (after Alzheimer's) and the most common movement disorder. Its pathologic hallmarks are the presence of Lewy bodies (LBs) containing misfolded fibrillary α-synuclein (α-syn) and the selective degeneration of midbrain dopaminergic (DA) neurons[1]. Increasing evidence has revealed that defective clearance of abnormal protein aggregates is central to the pathogenesis of PD. PD is characterized by both motor and non-motor symptoms and attacks millions of people worldwide, significantly affecting the life quality of patients. The current medical management of the disease is to alleviate symptoms while minimizing adverse drug effects. Development of disease-modifying drugs for PD is still an unmet challenge.

Macroautophagy (hereafter referred to as autophagy) is an evolutionarily conserved cellular process for degradation of cellular contents, including protein aggregates and damaged subcellular organelles, to maintain cellular homeostasis. Pharmacological modulation of autophagy has emerged as a promising strategy for the treatment of many diseases, including PD[2–4]. The phosphatidylinositol 3-kinase III (PI3KC3) complex, which consists of VPS34, VPS15 and Beclin 1 at its core, is the key signaling complex required for autophagosome formation and maturation. The synthesis of PI3P by the PI3KC3 complex on the phagophore allows the recruitment of additional autophagic components, thus promoting the expansion of the double membrane of the autophagosome as well as the fusion between autophagosome and lysosome. The PI3KC3 complex can be regulated by phosphorylation, ubiquitination, and interaction with its binding partners such as Bcl-2 and HMGB1, etc[5,6].

Uncaria rhynchophylla (Miq.) Jacks. (Gouteng in Chinese) is a traditional Chinese herbal medicine that is a component in a formula for the treatment of convulsions, hypertension, cerebral diseases and PD[7]. Previously, we identified a Beclin 1-dependent autophagy inducer, namely corynoxine B (Cory B) from Gouteng, which efficiently induced autophagy and promoted the clearance of α-syn in multiple cell models of PD[8,9]. Here, we report that Cory B promoted activity of the PI3KC3 complex and increased autophagy by directly binding to HMGB1/2. We found that HMGB2, a homolog of HMGB1, is also required for autophagy. Furthermore, we demonstrated the therapeutic activity of Cory B in fly and rodent models of PD, thereby suggesting its potential in the treatment of human PD.

2. Materials and methods

2.1. Reagents and antibodies

Reagents, antibodies, and their sources are shown in Supporting Information Table S1. Cory B (purity > 98%) was purchased from Aktin Chemicals, Inc. (Chengdu, China). The chemical structure of Cory B is shown in Fig. 1 below.

2.2. Cell culture

N2a cells were maintained in DMEM, supplemented with 10% FBS. PC12 cells were grown in DMEM, supplemented with 10% FBS and 5% horse serum. Transfection of DNA was performed using Lipo8000 or Lipofectamine 3000, and transfection of siRNA was performed using Lipofectamine 3000, both according to the manufacturer's instructions. EGFP-2xFYVE (#140047), RFP-GFP-LC3 (#21074), pCMV-VSV-G (#8454) and psPAX2 (#12260) plasmids were purchased from Addgene. RFP-LC3 (Mus) and Flag-Beclin 1 (Mus) plasmids were gifts from our cooperator. LentiCRISPRv2-HMGB1/2 and HMGB2-EGFP (C106S) (Mus) plasmids were constructed by us for this experiment.

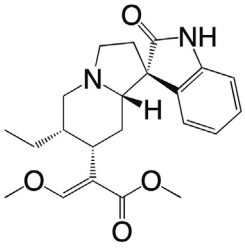

Figure 1 Structure of corynoxine B.

2.3. Animals, treatments, and sample preparation

Prp-α-Syn A53T transgenic mice were bought from Jackson's Lab (J004479) and maintained in a temperature-controlled (22 $\pm$ 2 °C) room on a 12 h light/dark cycle and given free access to food and water. All experimental procedures were conducted according to the Guide for the Care and Use of Laboratory Animals (National Institutes of Health) and approved by the University of Macau Animal Research Ethics Committee with ethical permit No. UMARE-018-2018. Every effort was made to minimize suffering and number of animals used. Pentobarbital was used to anesthetize the animals before they were terminated. Before one month of age, the newborn mice were genotyped by quantitative polymerase chain reaction to distinguish homozygous, heterozygous and wild-type (WT) mice according to the standard JAX protocol.

For the 2-month-old mice experiment, we selected 2-month-old heterozygous mice and WT littermates for our experiment. A53T α-syn heterozygous mice were randomly divided into two groups (n = 5, male). One group received intraperitoneal injection of Cory B dissolved in 10% Solutol HS 15 (20 mg/kg), the other group received control reagent (10% Solutol HS 15), daily for 1 month. For the 10-month-old mice experiment, we selected 10-month-old heterozygous mice and WT littermates. A53T α-syn heterozygous mice were randomly divided into four groups (n = 5, 2 male and 3 female). Three groups received intraperitoneal injection of different dosages of Cory B (5 mg/kg/day, 10 mg/kg/day and 20 mg/kg/day), while one group received control reagent (10% Solutol HS 15), for 1 month.

For the 15-month-old mice experiment, we selected 15-month-old heterozygous mice and WT littermates. A53T α-syn heterozygous mice were randomly divided into three groups (n = 8, female). Two groups were given different dosages of Cory B hydrochloride dissolved in saline (5 mg/kg; 20 mg/kg), and one group received control reagent (saline), once every 2 days for 2 consecutive months. All WT mice in the three experiments were given the corresponding control vehicle. For 15-month-old mice, behavior tests, constipation test and olfactory discrimination test were conducted during the last week. After finishing all the tests, mice were sacrificed and the brains were dissected for histology examination and biochemistry analysis. Each mouse brain was divided into two hemispheres. One half was fixed with 4% paraformaldehyde for immunostaining. The remaining half was divided into midbrain, prefrontal cortex, and other regions (three parts) and frozen at −80 °C.

2.4. Constipation test

As described before[10,11], animals were removed from their home cages and placed into a 12 cm × 25 cm translucent cylinder. Fecal pellets were counted over 15 min.

2.5. Olfactory discrimination test

This test is based on the fact that rodents usually prefer places impregnated with their own odor (familiar compartments), over places with other, non-familiar odors. The procedure was modified from the protocol reported by Rial et al.[12]. Briefly, each mouse was placed for 5 min in a cage divided into two equal areas separated by an open door. One compartment contained fresh sawdust (non-familiar compartment) while the other contained sawdust from its cage (familiar compartment). The mouse could freely choose where to spend time, and the time spent in each compartment was recorded.

2.6. Balance beam test

The balance beam test was used to test balance, muscle strength and motor coordination[13,14]. The procedure was modified from a previous report[14]. The balance beam is a square beam with a length of 1 m and a width of 12 mm. One end of the balance beam was placed in a black square box, and the mice were placed on the other end. The time that the mouse required to enter the black box by travelling on the beam was recorded within 60 s. The mice were given 3 trials of training, followed by three formal experiments with 30 min interval between each experiment. The average time was recorded.

2.7. Horizontal bar test

The procedure was adapted from a previous report[15]. The mouse's front paws were placed horizontally on a wooden rod with a diameter of 4 mm and a length of 40 cm firstly. Each end was supported by a pole 50 cm above the ground. The time the mice spent on the rod was recorded and their performance was scored according to this time as previously described[15]. After the testing using a 4 mm-diameter rod, the test was continued on a 6 mm-diameter rod after an interval of 30 min. The final performance score of the horizontal bar test was the sum of the two scores. Falls of mice caused by improper placement by the experimenter were not recorded.

2.8. Rotarod test

As described previously[15], the starting speed of the instrument was set to 4 RPM and the acceleration speed was 20 RPM. Ten seconds after placing the mouse on the rod, acceleration was started, and the speed at which the mouse fell off was recorded. The mice were acclimated to the training once and then underwent three consecutive tests of 5 min each. The rest time between each trial was above 30 min. The average speed at which the mice fell off the apparatus in three tests was used for analysis. Falls due to improper placement by the experimenter were not recorded.

2.9. Catwalk test

The CatWalk XT (Noldus) is a complete gait analysis system that can be used to quantitatively evaluate the footsteps and movement of mice[16,17]. It detects footprints by video-recording the animal from below while it traverses a glass plate, and uses Illuminated Footprints Technology (Noldus) to capture actual footprints. The mice were trained for three days before the formal experiment. The experiment was carried out according to the instructions that came with the equipment.

2.10. Drosophila culture

Drosophila flies were raised at 25 °C on standard corn meal medium supplemented with dry yeast. Cory B was dissolved in DMSO then diluted with water to desired concentrations. The drug-containing DMSO-water was added to instant drosophila food and mixed thoroughly. As the control, the same amount of DMSO in water alone was mixed with instant drosophila food. For

the treatment, larvae or adult flies were transferred to the medium and incubated for the indicated time.

2.11. Western blot analysis

Western blot was performed according to the method described previously[18]. In brief, total cell lysates or tissue homogenates (prefrontal cortex) were extracted in RIPA lysis buffer (Medium). To retrieve Triton X-100-soluble and -insoluble fraction, midbrains were homogenized in RIPA buffer [Tris-HCl 50 mmol/L pH 7.4, NaCl 175 mmol/L, EDTA 5 mmol/L pH 8.0, protease inhibitor cocktail] containing 1% Triton X-100, and centrifuged at 15,000 × *g* for 60 min at 4 °C. Triton X-100 insoluble proteins were found in the precipitate; soluble proteins were in the supernatant. The insoluble fraction was solubilized in lysis buffer containing 2% SDS[19]. Protein concentration was determined using a BCA kit. An equal amount of protein was separated by SDS-PAGE and transferred onto PVDF membrane. The nonspecific binding was blocked by 5% nonfat milk in TBST. The membranes were incubated with primary antibodies overnight at 4 °C, and then incubated with HRP-conjugated secondary antibodies for 2 h at room temperature. The protein signals were visualized by ECL and detected by ChemiDoc MP Imaging System (Bio-Rad).

2.12. Co-IP analysis

Co-IP was performed according to the method described previously[20]. In brief, cells were homogenized in RIPA lysis buffer (Weak). Protein concentration was determined using a BCA kit. An equal amount of protein was incubated with anti-Flag magnetic beads overnight. The beads, including the protein that was pulled down, were washed with IP lysis buffer, denatured in 1 × sample loading buffer, and separated by SDS-PAGE. Clean-Blot IP Detection Kit was used to detect functional primary antibodies, HMGB1 and HMGB2.

2.13. SILAC labeling and sample preparation

SILAC labeling was done according to the instructions provided by Thermo Scientific. According to the weights of the labeled essential amino acids, N2a cells were divided into two groups: "heavy" ($^{13}C_6$ $^{15}N_2$ L-lysine-2HCl and $^{13}C_6$ $^{15}N_4$ L-arginine-HCl) and "light" (L-lysine-2HCl, L-Arginine-HCl). Each group of N2a cells was grown over 6 generations in "light" and "heavy" SILAC media to allow full incorporation of amino acids into proteins. The "light" and "heavy" groups were transfected with Flag-Beclin 1 and then treated with DMSO or Cory B for 6 h. The cell lysates were mixed at a ratio of 1:1 and co-IP were subjected to pull-down with anti-Flag magnetic beads and analyzed by LC−MS/MS.

2.14. siRNA-mediated knockdown assay

siRNA transfection into N2a cells was performed using Lipofectamine 3000 according to the manufacturer's instructions. At 48 h after transfection, the cells were used for experiments.

Hmgb1 siRNA sequence (sense 5′−3′): GGCUGACAA GGCUCGUUAU;

Hmgb2 siRNA sequence (sense 5′−3′): GCAGAAAG CAGCUAAACUATT.

2.15. Immunofluorescence staining

Immunofluorescence staining for HMGB1 and HMGB2 was performed according to a previously described method to determine their localization in cells[5]. Cells after different treatments were fixed in 4% PFA, blocked with 1% BSA, and incubated with specific primary antibodies of HMGB1 and HMGB2 overnight at 4 °C. After being rinsed three times with PBS, the cells were incubated with Alexa Fluor 555-labeled anti-rabbit IgG for 2 h at 37 °C. The nuclei were stained with Hoechst 33,342, and the slides were sealed and visualized by LSM 880 with Airyscan (Zeiss). For drosophila and mouse brains, fixed tissues were treated with PBST (0.3% Triton X-100 in PBS) for 10 min before immunostaining as described above.

2.16. Cellular thermal shift assay (CETSA)

Binding between Cory B and target proteins in cells was analyzed by CETSA according to the method described previously[21]. In brief, cells were treated with FBS-free medium with or without 200 μmol/L Cory B for 1 h. After sample collection, cells were washed and resuspended in 1 mL PBS, followed by three freeze-thaw cycles to obtain cytoplasmic components. Pairs consisting of one control aliquot and one experimental aliquot were heated at 41.4 °C, 44 °C, 47.6 °C, 50.5 °C, 53.4 °C, 56.5 °C, 59.1 °C, 62.2 °C, 65.6 °C, or 69 °C for 3 min. Following centrifugation at 12,500 RPM (CT5RE, Hitachi Koki, Tokyo, Japan) for 30 min at 4 °C, supernatants were collected. Western blot was used to detect the degradation of indicated proteins under various temperatures, and the degradation curves of control group and treatment group were obtained for comparison.

2.17. Surface plasmon resonance (SPR) analysis

In brief, CM5 sensor chip was immobilized by recombinant human HMGB1/2 protein. Cory B at various concentrations were diluted with running buffer (1 × PBS with 0.05% Tween-20, pH 7.4, 5% DMSO), and injected into the fluid flow system at a flow rate of 30 μL/min for a 60 s association phase, followed by 90 s dissociation phase. Both association and dissociation processes were handled in the running buffer.

2.18. Generation of Hmgb1/2 knockout N2a cells by CRISPR-Cas9

sgRNA (TCATACTCACGGAGGCCTCT)-targeting murine *Hmgb1* and sgRNA (CCCATAGACCATGTCTGCAA)-targeting murine *Hmgb2* were chosen according to Zhang's publication[22]. Lentiviral vector was constructed by cloning the target sequence into the lentiCRISPRv2 backbone by standard protocol. To prepare the lentivirus, HEK293T cells were transiently transfected with a lentiviral vector, together with pCMV-VSV-G and psPAX2 using Lipofectamine 3000. After cells were cultured for 2−3 days, the supernatant was collected and passed through a 0.45-μm syringe filter unit. Cells were cultured with lentivirus and 8 μg/mL polybrene, and stable transformants were selected with puromycin.

2.19. Immunohistochemistry tests

Immunohistochemistry tests were performed according to the method described previously[18]. In brief, frozen brain tissues

containing midbrain were cut into 20 μm-thick sections by Leica CM1950 (Leica); sections were stained with purified anti-α-syn phospho-(Ser129) antibody. Sections were washed with PBS; then 3% H_2O_2 was added to remove endogenous hydrogen peroxidase. Then sections were blocked with PBST (0.1% TritonX-100 in PBS)-diluted goat serum (10%) for 1 h. Next, they were incubated at 4 °C with anti-α-syn phospho-(Ser129) antibody overnight. Finally, the slices were sequentially incubated with HRP-conjugated anti-mouse secondary antibody for 2 h and visualized with DAB. The results were evaluated by light microscope ECLIPSE Ci-L (Nikon) and photographed with a digital camera.

2.20. Statistical analysis

The data were expressed as mean ± standard deviation (SD) or mean ± standard error of mean (SEM). One-way ANOVA was used for multiple comparisons, and *t*-test was used to analyze the differences of measurement variables between two groups. Data were analyzed with GraphPad Prism 8 or IBM SPSS Statistics 23 and considered statistically significant at $P < 0.05$.

3. Results

3.1. Cory B activated PI3KC3 and increased the interaction between HMGB1/2 and Beclin 1

Our preliminary study found that Cory B is a neuronal autophagy inducer, which induces autophagy in a Beclin 1-dependent but mTOR-independent manner[8,9]. In this study, PC12 cells were firstly transfected with EGFP-2xFYVE, a probe of PI3P, and then treated with SAR405 or Cory B. SAR405 is a strong PI3KC3 inhibitor. The results showed that Cory B significantly increased the formation of EGFP-2xFYVE puncta in PC12 cells ($P < 0.001$) (Fig. 2A and B). Similarly, in EGFP-2xFYVE- and RFP-LC3-overexpressing N2a cells, Cory B significantly increased the formation of EGFP-2xFYVE puncta and EGFP-2xFYVE colocalization with RFP-LC3, suggesting PI3KC3 activation on autophagic structures (Fig. 2C−E). The total expression levels of VPS34, Atg14 L, Beclin 1 proteins did not change after Cory B treatment, suggesting that Cory B activated PI3KC3 in a translation-independent manner. AMPK, another important autophagy-initiating kinase, was also not induced by Cory B (Supporting Information Fig. S1).

To determine whether Cory B regulates PI3KC3 activity by modulating its interaction with binding partners, we used stable isotope labeling by amino acids in cell culture (SILAC)-coupled LC−MS/MS to quantitatively analyze the Flag-Beclin 1 interactome in Flag-Beclin 1-expressing N2a cells, both those with and without 20 μmol/L Cory B treatment for 6 h (Fig. 2F). MS data showed that much more HMGB1, a reported autophagy regulatory protein, was pulled down by Flag beads after Cory B treatment. Interestingly, more HMGB2, the homolog of HMGB1, was also pulled down by Flag beads in the Cory B-treated group (Fig. 2G). We further performed IP experiments to confirm that the interaction between Beclin 1 and HMGB1/HMGB2 was enhanced after Cory B treatment, while the binding of VPS34 and Atg14 L to Beclin 1 were unchanged (Fig. 2H and I). These results suggest that Cory B may activate PI3KC3 by increasing the interaction between HMGB1 and Beclin 1; however, whether HMGB2 plays the same role as HMGB1 in autophagy remains unknown.

3.2. HMGB1/2 acted as a target for cory B to promote autophagy

It has been reported that cytoplasmic HMGB1 induces autophagy by directly interacting with Beclin 1 to displace Bcl-2. Under normal conditions, only 5%−10% of HMGB1 protein is located in the cytosol, with the specific quantity dependent on the cell type[5]. Here, by immunostaining, we observed a significant increase in cytoplasmic HMGB1 content ($P < 0.001$) and its co-location with EGFP-2xFYVE after Cory B treatment, indicating that Cory B induced HMGB1 cytoplasmic translocation and promoted Beclin 1-VPS34 complex formation (Fig. 3A, C and E). Interestingly, HMGB2 showed the same change after Cory B treatment (Fig. 3B, D and F). To confirm whether HMGB1 mediated Cory B-induced autophagy, we first constructed *Hmgb1* knockout cells, and then added Cory B to detect autophagy level. It can be seen that Cory B-induced autophagy was only partially blocked in *Hmgb1* knockout cells. Interestingly, after siRNA-mediated depletion of HMGB2 in *Hmgb1* knockout cells, Cory B-induced autophagy was largely abolished (Fig. 3G−I). In addition, we examined the effects of Cory B on autophagy after knocking down *Hmgb1*, *Hmgb2*, or both in N2a cells by siRNA. The individual knockdown of *Hmgb1* or *Hmgb2* markedly inhibited Cory B-induced autophagy in N2a cells, and dual knockdown of *Hmgb1* and *Hmgb2* synergistically enhanced the inhibitory effect (Supporting Information Fig. S2). These results indicate a crucial role of both HMGB1 and HMGB2 in Cory B-induced autophagy.

3.3. HMGB2 was required for PI3KC3 activity and autophagy induction

Knockdown of HMGB2 impaired Cory B-induced autophagy (Fig. 3G−I), and here we further demonstrated this in *Hmgb2* KO N2a cells. Results show that Cory B-induced autophagy can be partially blocked in *Hmgb2* knockout cells, decreasing Cory B-induced LC3II formation and p62 degradation (Fig. 4A−C).

To confirm the role of HMGB2 in autophagy, autophagy flux was detected by tandem RFP-GFP-LC3 reporter and LC3-II turnover assay (LC3-II level with late-stage autophagy inhibitors) according to the AMSS: autophagy characterization assay both in WT and *Hmgb2* KO N2a cells in basal and autophagy-inducing states[23]. In RFP-GFP-LC3-overexpressing cells, we can see that the red-only puncta were significantly reduced in *Hmgb2* KO cells ($P < 0.001$) (Fig. 4D and E). Western blot analysis showed that endogenous LC3-II expression was significantly decreased in *Hmgb2* KO N2a cells compared with WT N2a cells ($P < 0.01$), especially after treatment with autophagy inducer Torin 1 (Fig. 4F and G) ($P < 0.001$). LC3-II levels in the different stimulus and CQ co-treatment group were much higher than in CQ-alone treatment group, and, compared with WT N2a, the corresponding accumulation of LC3II in *Hmgb2* KO N2a cells was much less (Fig. 4F and H). Next, we co-transfected RFP-LC3 and EGFP-2xFYVE in WT and *Hmgb2* KO N2a cells, and then added EBSS or Torin 1 for 4 h. The results showed that increased formation of RFP-LC3 puncta and EGFP-2xFYVE puncta, as well as their colocalization, could be significantly blocked by *Hmgb2* depletion ($P < 0.01$) (Fig. 4I−K). Collectively, these results indicate a positive role of HMGB2 in PI3KC3 activation and autophagy regulation.

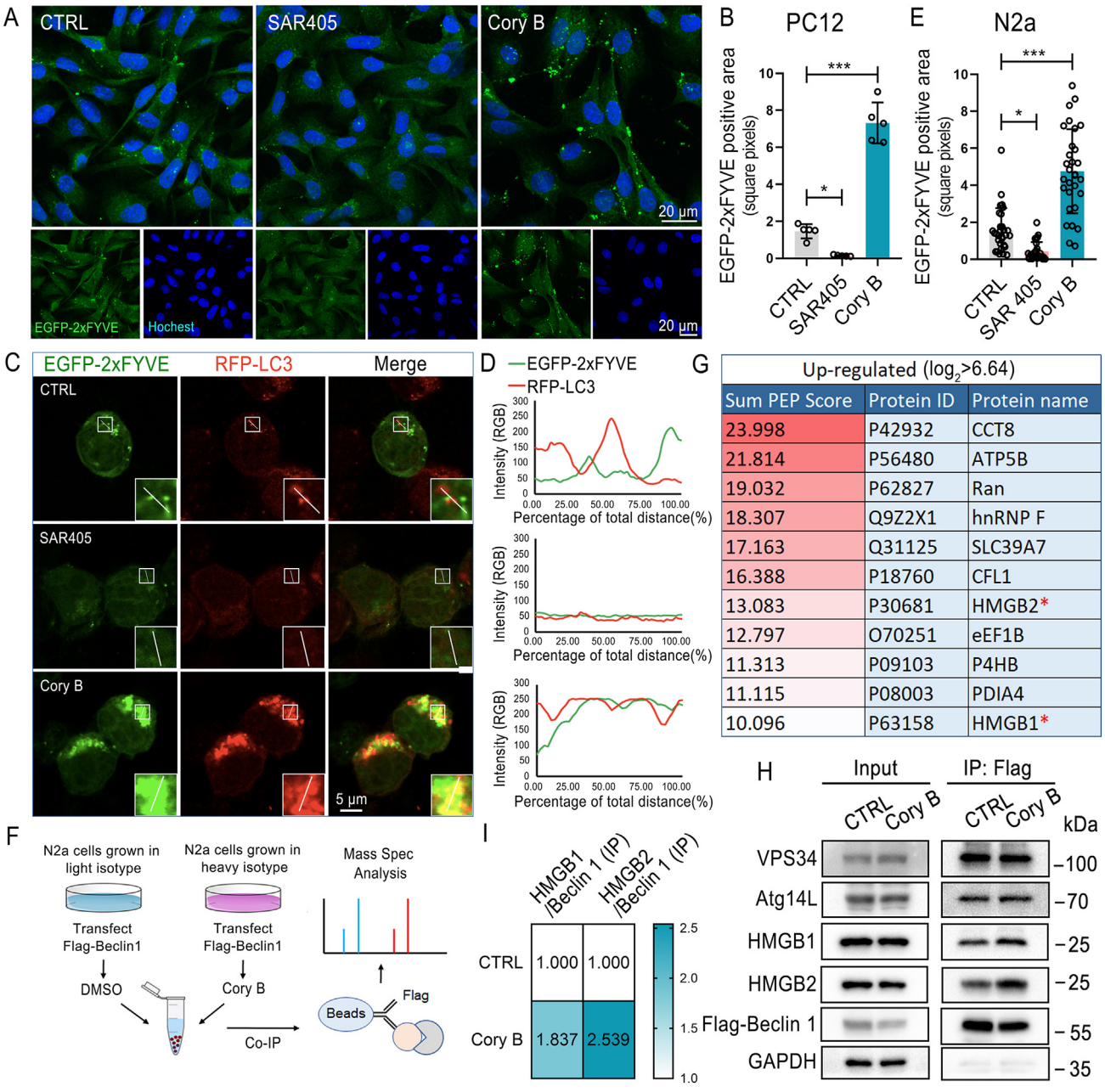

G

Up-regulated (log_2>6.64)		
Sum PEP Score	Protein ID	Protein name
23.998	P42932	CCT8
21.814	P56480	ATP5B
19.032	P62827	Ran
18.307	Q9Z2X1	hnRNP F
17.163	Q31125	SLC39A7
16.388	P18760	CFL1
13.083	P30681	HMGB2*
12.797	O70251	eEF1B
11.313	P09103	P4HB
11.115	P08003	PDIA4
10.096	P63158	HMGB1*

Figure 2 Corynoxine B (Cory B) activated phosphatidylinositol 3-kinase III and increased the interaction between HMGB1/2 and Beclin 1. (A) EGFP-2xFYVE-transfected PC12 cells were treated with 1 μmol/L SAR405 or 20 μmol/L Cory B for 6 h. Fluorescence was observed under a confocal microscope, and representative figures are shown. (B) Quantification of EGFP-2xFYVE-positive area in PC12 cells. $n > 250$ cells from 5 fields were analyzed. (C, D) EGFP-2xFYVE and RFP-LC3 co-transfected N2a cells were treated with 1 μmol/L SAR405 or 20 μmol/L Cory B for 12 h. Fluorescence was observed under a confocal microscope, and representative figures are shown. The results of co-localization were analyzed by Leica Application Suite X and EXCEL software. (E) Quantification of EGFP-2xFYVE positive area in N2a cells. $n = 30$ cells. (F) Workflow of SILAC-coupled LC−MS/MS identification of Flag-Beclin 1 interactome. (G) Upregulated binding proteins after Cory B treatment. (H, I) Flag-Beclin 1-transfected N2a cells with and without 20 μmol/L Cory B treatment for 6 h; subsequently subjected to co-IP with anti-Flag magnetic beads and detected with VPS34, Atg14 L, Beclin 1, HMGB1, HMGB2 antibodies. All data are presented as mean ± SD. $^*P < 0.05$, $^{***}P < 0.001$, one-way ANOVA for multiple comparison and Tukey's test as *post hoc* test.

3.4. *Cory B directly bound to HMGB1 and HMGB2*

Small molecule-protein target engagement is a critical step for understanding the mechanism of a drug's action and the biology of disease-relevant targets. To determine whether Cory B directly binds to HMGB1/2, we used CETSA to perform label-free target validation; CETSA is based on the principle that ligand binding enhances the thermal stability of target proteins (Fig. 5A)[21,24]. We found that the thermal stability of HMGB1/2 in Cory B-treated N2a cell lysates was increased compared with the control group (Fig. 5B). By plotting the relative intensity of HMGB1, HMGB2 or β-actin against temperatures to generate thermal melting

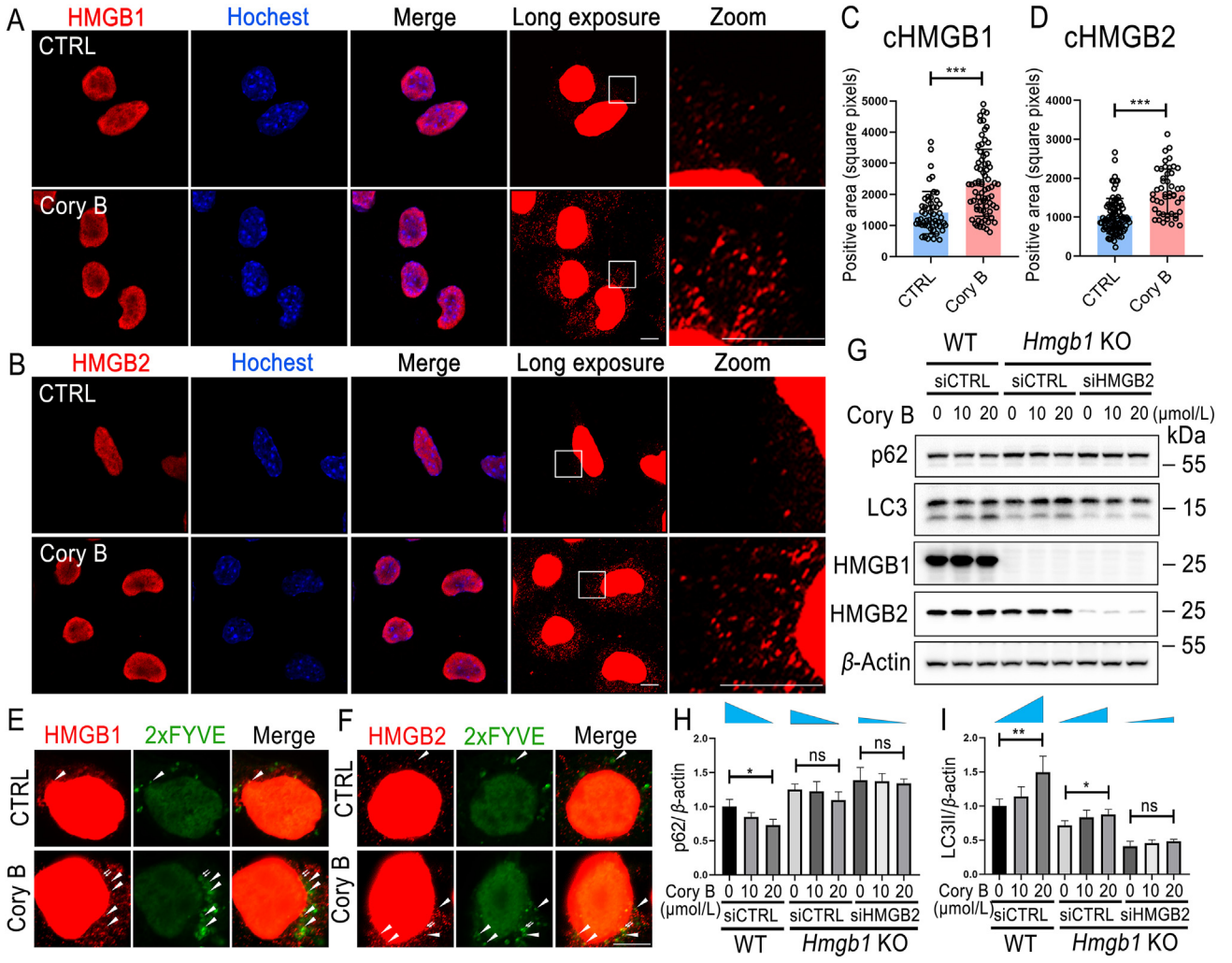

Figure 3 HMGB1/2 acted as a target for corynoxine B (Cory B) to promote autophagy. (A, B) N2a cells were treated with 20 μmol/L Cory B for 6 h and immunostained with the indicated antibodies and Hoechst. Fluorescence was observed under Zeiss LSM800 with Airyscan, and representative figures are shown. Scale bar = 5 μm. (C, D) Quantification of cytoplasmic HMGB1/2 (cHMGB1/2) positive area in each group. $n > 45$ cells. (E, F) EGFP-2xFYVE-transfected N2a cells were treated with 20 μmol/L Cory B for 6 h and immunostained with the indicated antibodies. Fluorescence was observed with a Zeiss LSM800 microscope with Airyscan, and representative figures are shown. Arrows indicate colocalizations of HMGB1 and PI3P. Scale bar = 5 μm. (G) Wildtype (WT) N2a cells were transfected with non-target siRNA (siCTRL), and *Hmgb1* knockout (KO) N2a cells were transfected with non-target siRNA and HMGB2-specific siRNA (siHMGB2) for 24 h followed by indicated concentration of Cory B treatment for another 6 h. Cell lysates were subjected to Western blot analysis. (H, I) Normalized band intensities of p62/β-actin and LC3II/β-actin from three independent experiments. The slope direction of each blue triangle represents the trend of change, and the magnitude of the angle in this direction represents the magnitude of the trend. All data are presented as mean ± SD. $^{*}P < 0.05$; $^{**}P < 0.01$; $^{***}P < 0.001$; ns, no significance; one-way ANOVA for multiple comparison and Tukey's test as *post hoc* test.

curves, we observed an obvious shift in the HMGB1/2 curve of Cory B-treated N2a cell lysates compared with control cell lysates, while the curves of β-actin were barely changed. This indicates that Cory B directly binds to HMGB1/2 in cells (Fig. 5D−F). Interestingly, the thermal stability of Beclin 1 did not change after 1 h of Cory B treatment, implying that Cory B binding to HMGB1/2 may be an upstream event prior to Beclin 1 involvement (Supporting Information Fig. S3).

Surface plasmon resonance (SPR) biosensing provides direct binding information as well as real time kinetic data. In the study, purified HMGB1 protein and HMGB2 protein were fixed on the chips through covalent bonds, and the solutions containing Cory B flowed through the chip, giving us a chance to monitor the binding energy. Titration results revealed that Cory B can bind to both HMGB1 and HMGB2. The K_D of Cory B and HMGB1 protein was 150 ± 10 μmol/L (Fig. 5I and J). The K_D of Cory B and HMGB2 protein was 210 ± 10 μmol/L (Fig. 5K and L).

To understand the binding pattern of Cory B and HMGB 1/2, we applied molecular docking to predict the binding site of Cory B with HMGB1/2. The cavity of Cory B in HMGB1 is composed of K88, F89, K90, K96, R97, P98, P99, S100, and F103, while the cavity of Cory B in HMGB2 is similar to that in HMGB1, where the pocket is composed of K88, K90, R97, P98, S100, F103, and K152 (Fig. 5M−P). Given that C106 of HMGB1 is critical in determining the translocation of HMGB 1 between the nucleus and cytoplasm[5], and that HMGB1/2 have similar structures and binding patterns with Cory B near site C106, we hypothesized that Cory B promotes the translocation of HMGB1/2 to induce

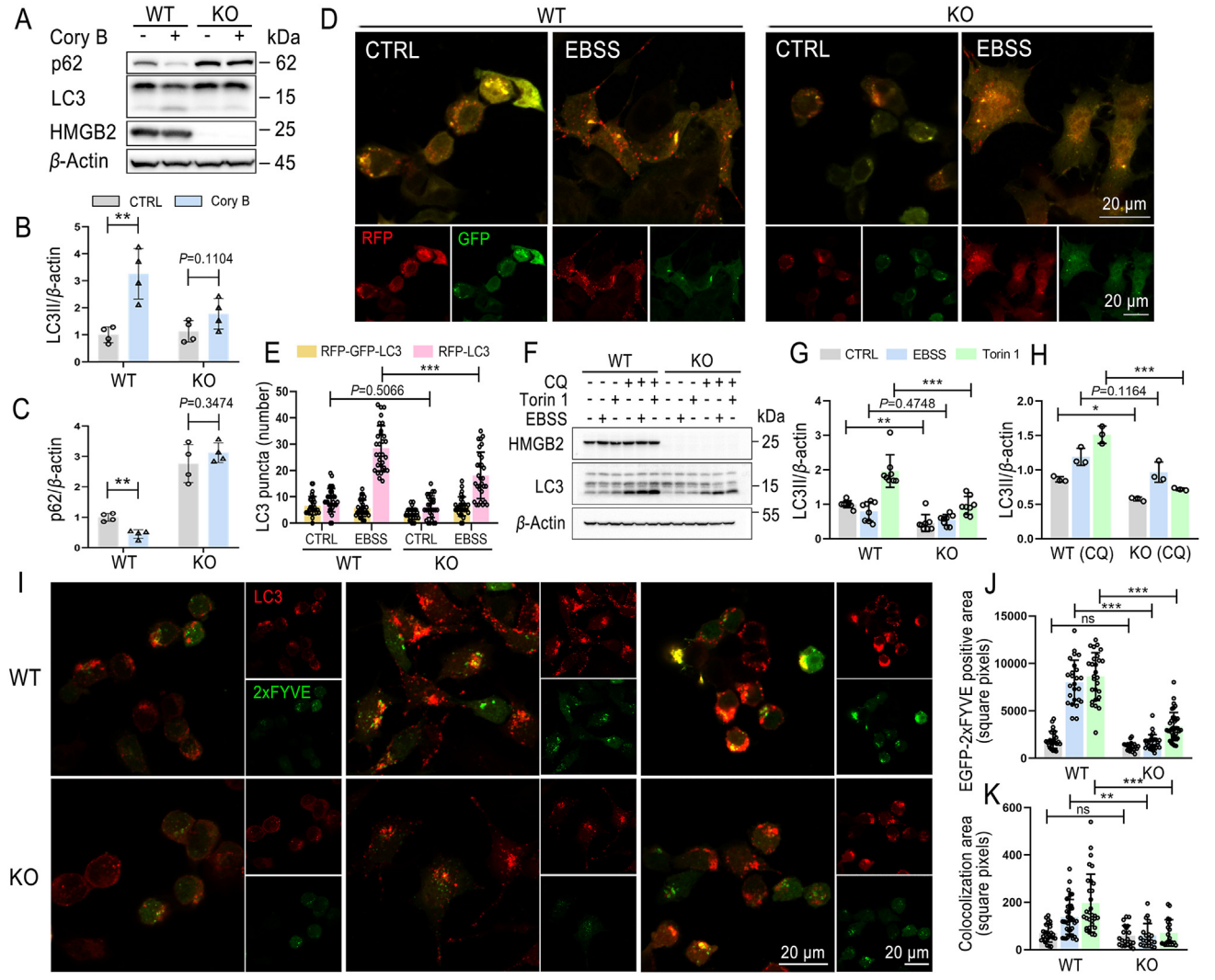

Figure 4 HMGB2 was required for phosphatidylinositol 3-kinase III activity and autophagy induction. (A−C) Wildtype (WT) N2a cells and *Hmgb2* knockout (KO) N2a cells were treated with 20 μmol/L corynoxine B (Cory B) for 6 h. Expression levels of LC3II and p62 were assessed by Western blot, and quantifications are shown. (D, E) RFP-GFP-LC3-transfected N2a cells and *Hmgb2* KO N2a cells were untreated or treated with Earle's balanced salt solution (EBSS) for 6 h. Fluorescence was observed under a confocal microscope, and representative figures are shown. Quantification of LC3 puncta numbers is shown. $n = 30$ cells per group. (F−H) WT N2a cells and *Hmgb2* KO N2a cells were treated with EBSS or 1 μmol/L Torin 1 alone or cotreated with chloroquine (CQ) for 6 h. Expression level of LC3II was assessed by Western blot, and quantifications are shown. (I−K) EGFP-2xFYVE and RFP-LC3 co-transfected N2a cells or *Hmgb2* KO N2a cells were untreated or treated with EBSS or 1 μmol/L Torin1 for 6 h. Fluorescence was observed under a confocal microscope, and representative figures are shown. Quantification of RFP-LC3 and EGFP-2xFYVE positive aera are shown. $n > 20$ cells per group. All data are presented as mean ± SD. $^*P < 0.05$; $^{**}P < 0.01$; $^{***}P < 0.001$; ns, no significance; one-way ANOVA for multiple comparison and Tukey's test as *post hoc* test.

autophagy by direct binding. When we overexpressed HMGB2 (C106S) in *Hmgb2* KO cells, we found that HMGB2 (C106S) can also bind to Cory B (Fig. 5C, G and H), suggesting that mutations at this site do not affect its binding to Cory B but may affect its role in autophagy.

3.5. *Cory B induced autophagy and prevented neurodegenerative phenotypes in drosophila*

As the major nutrient storage organ of the drosophila larvae, the fat body is naturally sensitive to nutrient starvation and elicits a robust autophagic burst upon autophagic stimulus. In our study, GFP-Atg8a-overexpressing drosophila larvae were fed Cory B for 6 h, and then their fat bodies were isolated for observation. We found that Cory B induced the formation of GFP-Atg8a puncta in drosophila fat bodies, suggesting the autophagy had been induced (Fig. 6A). In α-syn transgenic flies, Cory B decreased the α-syn levels and prevented the neurodegenerative phenotypes of PD, including loss of tyrosine hydroxylase-positive dorsomedial dopamine neurons ($P < 0.01$) and impaired motor function ($P < 0.05$) (Fig. 6B−E), revealing the protective role of Cory B in this drosophila model of PD.

3.6. *Cory B promoted α-syn clearance in transgenic mice of different ages*

To test the therapeutic effects of Cory B in eliminating α-syn pathology in the brain, A53T α-syn heterozygous transgenic PD

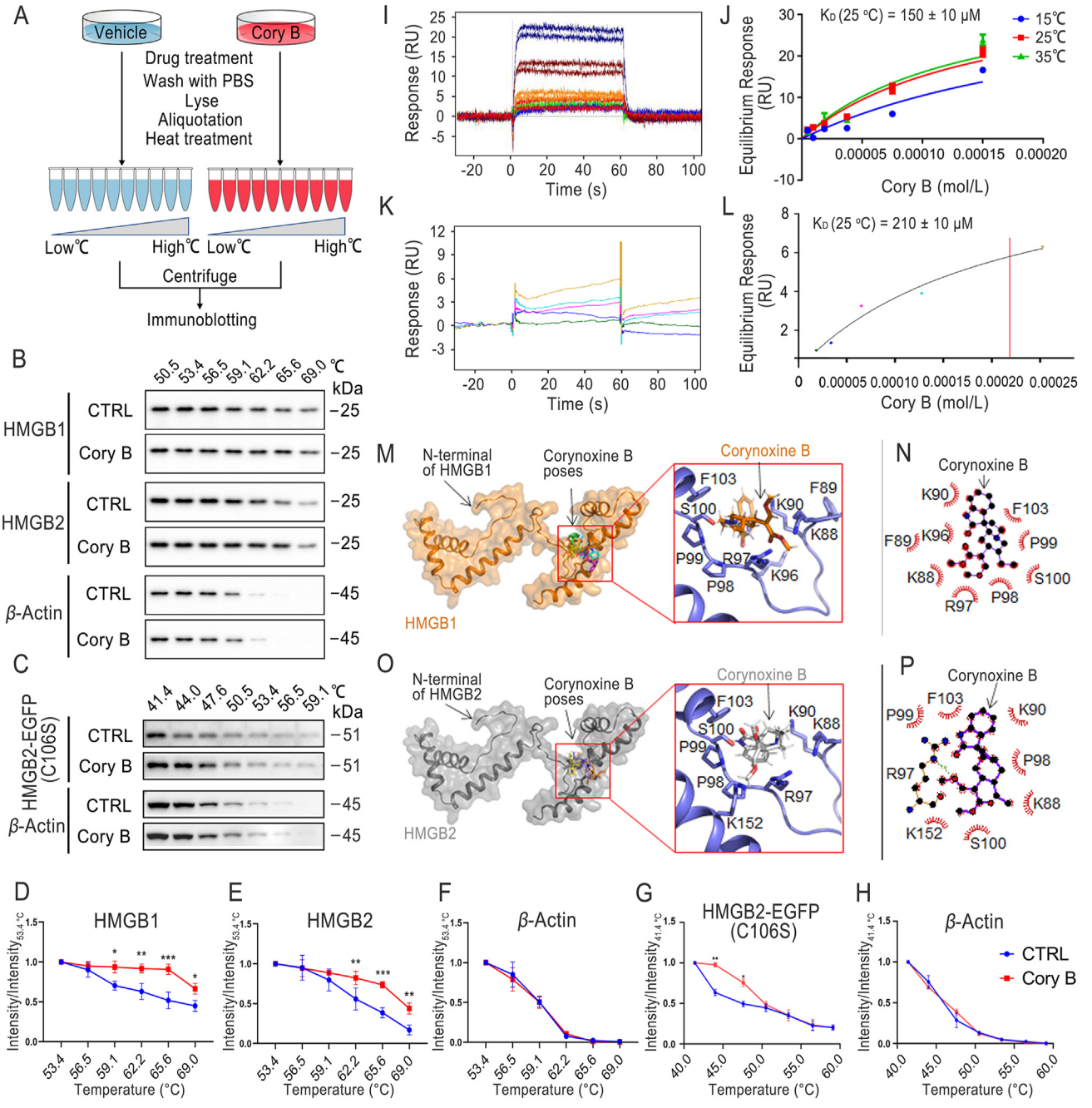

Figure 5 Corynoxine B (Cory B) directly bound to HMGB1 and HMGB2. (A) Workflow of a CETSA for HMGB1/2 in intact cells. (B) CETSA was performed in N2a cells. Cell lysates in control group and Cory B treatment group were subjected to Western blot analysis. (C) CETSA was performed in HMGB2-EGFP (C106S)-overexpressed *Hmgb2* knockout N2a cells. Cell lysates in control group and Cory B treatment group were subjected to Western blot analysis. (D−F) CETSA curves of HMGB1, HMGB2 or β-actin in N2a cells were determined in the absence and presence of Cory B. Normalized band intensity ratios from three independent experiments are presented as mean ± SD (*$P < 0.05$, **$P < 0.01$, ***$P < 0.001$). (G, H) CETSA curves of HMGB2-EGFP (C106S) or β-actin in HMGB2-EGFP (C106S)-overexpressed *Hmgb2* knockout N2a cells were determined in the absence and presence of Cory B. Normalized band intensity ratios from three independent experiments are presented as mean ± SD (*$P < 0.05$, **$P < 0.01$). (I, J) SPR titration curve and dose-response plot of the Cory B-HMGB1 binding. (K, L) SPR titration curve and dose-response plot of the Cory B-HMGB2 binding. (M) Docking poses of Cory B-HMGB1 binding. The homology model of HMGB1 is shown in orange ribbon and surface. The docking score of Cory B binding to HMGB1 ranked in top 5 poses were selected. The poses are superimposed and shown in licorice. The cavity of Cory B in HMGB1 was composed of K88, F89, K90, K96, R97, P98, P99, S100, and F103. (N) Schematic representation of interactions between Cory B and HMGB1 analyzed by LigPlot+program. (O) Docking poses of Cory B-HMGB2 binding. The receptor HMGB2 is displayed in grey ribbon and surface, while the top 5 ligand poses were superimposed and shown in licorice. The cavity of Cory B in HMGB2 is similar to that in HMGB1. The pocket is composed of K88, K90, R97, P98, S100, F103, and K152. (P) Schematic representation of Cory B interaction with HMGB2. The green dashed line indicates a hydrogen bond formed between R97 of HMGB2 and Cory B.

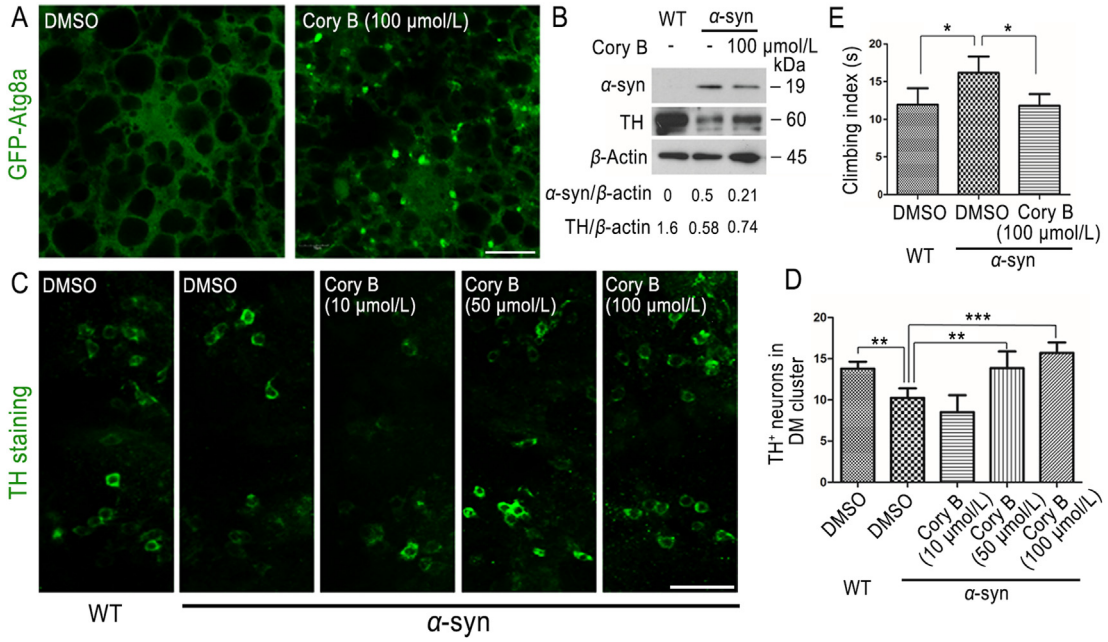

Figure 6 Corynoxine B (Cory B) induced autophagy and prevented neurodegenerative phenotypes in drosophila. (A) GFP-Atg8a-overexpressing (Cg-GAL4+; UAS-GFP-Atg8a) drosophila larvae (96 h after egg laying) were fed with 100 μmol/L Cory B dissolved in instant fly food for 6 h, and the fat bodies were isolated for observation under a fluorescence microscope. Scale bar = 20 μm. (B) 0−3-day-old flies (Elav-GAL4/+, Elav-GAL4/+; α-synuclein (α-syn) wildtype (WT)/+) were used. Flies were treated with 100 μmol/L Cory B or DMSO for 25 days, and fly heads were collected for WB. Expression levels of α-syn and tyrosine hydroxylase (TH) were assessed. (C, D) Administration of Cory B rescued α-syn-mediated toxicity of dorsomedial (DM) dopamine neurons in 28-day-old transgenic flies in a dose-dependent manner. Fluorescence was observed under a fluorescence microscope, and representative figures are shown. Scale bar = 40 μm. (E) 0−3-day-old flies (Ddc-GAL4/+, Ddc-GAL4/+; α-syn WT/+) were used. Climbing test was performed after flies were treated with 100 μmol/L Cory B or DMSO for 25 days. Above quantifications are shown as mean ± SEM (*$P < 0.05$, **$P < 0.01$, ***$P < 0.001$).

mice aged 2, 10 and 15 months were intraperitoneally injected with Cory B or control solvent as described in the methods section. The prefrontal cortex and midbrain of mice in different groups were sequentially extracted with buffers with increasing strength of protein solubilization to separate the soluble and insoluble fractions. Western blot was used to detect α-syn in different lysate extracts. The results showed that both Triton-X100-soluble and -insoluble α-syn significantly increased in transgenic mice, and its level decreased consistently after Cory B treatment in a dose-dependent manner ($P < 0.05$) in all age groups (Fig. 7A−H, K and L). In addition, we performed immunostaining to detect phospho-(Ser129) α-syn in midbrain and visualized α-syn pathology in tyrosine hydroxylase-positive neurons of 15-month-old mice. The results were consistent with the WB results, *i.e.*, that Cory B reduced phospho-(Ser129) α-syn and α-syn in TH neurons (Fig. 7I, Supporting Information Fig. S4A).

3.7. Cory B improved behavioral performance in 15-month-old PD transgenic mice and induced autophagy in vivo

The α-syn transgenic PD mice models do not display motor phenotypes until they age[25], so we selected mice aged 15 months to observe the therapeutic effect of Cory B on PD-related behavior phenotypes and the autophagy levels in the brain. Fig. 8A shows the experimental process. Administration of Cory B was safe, and the mice showed normal weight change compared with mice that had received vehicle (Fig. 8B). Over the course of PD progression, motor impairments are generally preceded by nonmotor symptoms (NMS) including decreased GI function and constipation in the early stages of disease[26]. Here, we detected early behavioral changes through olfactory discrimination test and constipation test as described in Materials and Methods. In transgenic animals, we observed a significant decrease in the total output of fecal pellets and an increase after Cory B treatment ($P < 0.01$) (Fig. 8C). Similarly, olfactory defects were observed in mice in model groups and alleviated in Cory B-treated mice, although there was no significant difference (Fig. 8D). These data reflect a favorable improvement in the recovery of early NMS dysfunction after Cory B treatment.

Fine motor coordination and balance of mice were measured *via* four tests: balance beam test, rotarod test, horizontal bar test and CatWalk gait test, as described in the Materials and Methods. 15-month-old α-syn-overexpressing mice required significantly more time to cross the challenge beam ($P < 0.01$) and also exhibited worse performance in the horizontal bar test ($P < 0.05$) and rotarod test compared to WT littermates. Cory B treatment markedly reduced the defects of PD mice in the balance beam and horizontal bar tests ($P < 0.05$), and slightly alleviated the defects affecting the rotarod test (Fig. 8E−G). In the CatWalk gait test, since there was no significant difference in movement speed or body weight between WT mice and α-syn transgenic mice in our observation, we compared the parameters reflecting the walking posture (gait) of mice. Swing (s) is the duration in seconds of no contact of a paw with the glass plate. Swing Speed is the speed (Distance Unit/second) of the paw during Swing, which can be used to reflect steps of walking. Print position is defined as the distance between the position of the hind paw and the position of the previously placed front paw on the same side of the body

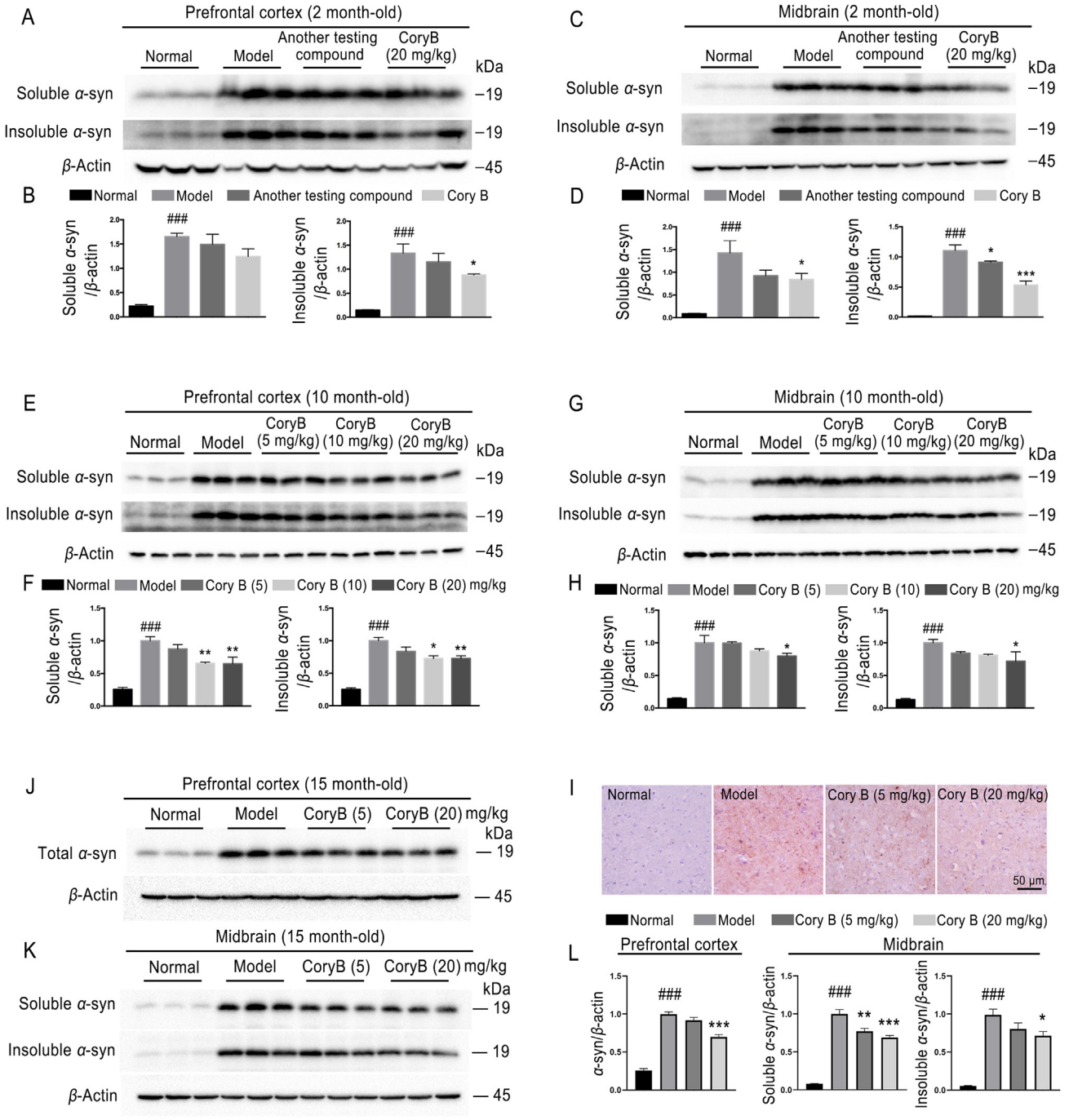

Figure 7 Corynoxine B (Cory B) promoted α-synuclein (α-syn) clearance in 2-, 10- and 15-month-old transgenic mice. (A−H, K, L) Prefrontal cortexes and midbrains of 2- and 10-month-old mice, and the midbrain of 15-month-old mice were sequentially extracted with Triton-X100-soluble and -insoluble buffers, as described in Materials and Methods. The expression levels of α-syn in each fraction were analyzed by Western blot. (J, L) Prefrontal cortexes of 15-month-old mice were extracted with RIPA lysis buffer (Medium) for Western blot analysis. Expression level of α-syn was assessed. (I) Representative images of α-syn pathology in the midbrain of 15-month-old mice in different groups immunolabeled with anti-α-synuclein phospho-(Ser129) antibody. Above quantifications are shown as mean ± SEM ($^{###}P < 0.001$ *vs.* normal group; $^{*}P < 0.05$, $^{**}P < 0.01$, $^{***}P < 0.001$ *vs.* model group, $n = 5$ mice).

(ipsilateral) and in the same step cycle. We can see that the PD model mice have significant changes in these two parameters, and these changes were reversed by Cory B (Fig. 8H and I). Taken together, results of motor tests revealed an improvement of abnormal motor behavior of α-syn A53T mice treated with Cory B compared to vehicle-treated α-syn A53T controls.

To determine the autophagy level in mice brain, we detected the expression of p62 and LC3 in brain lysate by Western blot, and found that the content of p62, ordinarily increased in PD mouse brain tissue, decreased after cory B treatment ($P < 0.05$). The level of LC3II also increased after Cory B treatment ($P < 0.001$) (Fig. 8J−L), indicating autophagosome formation is promoted by

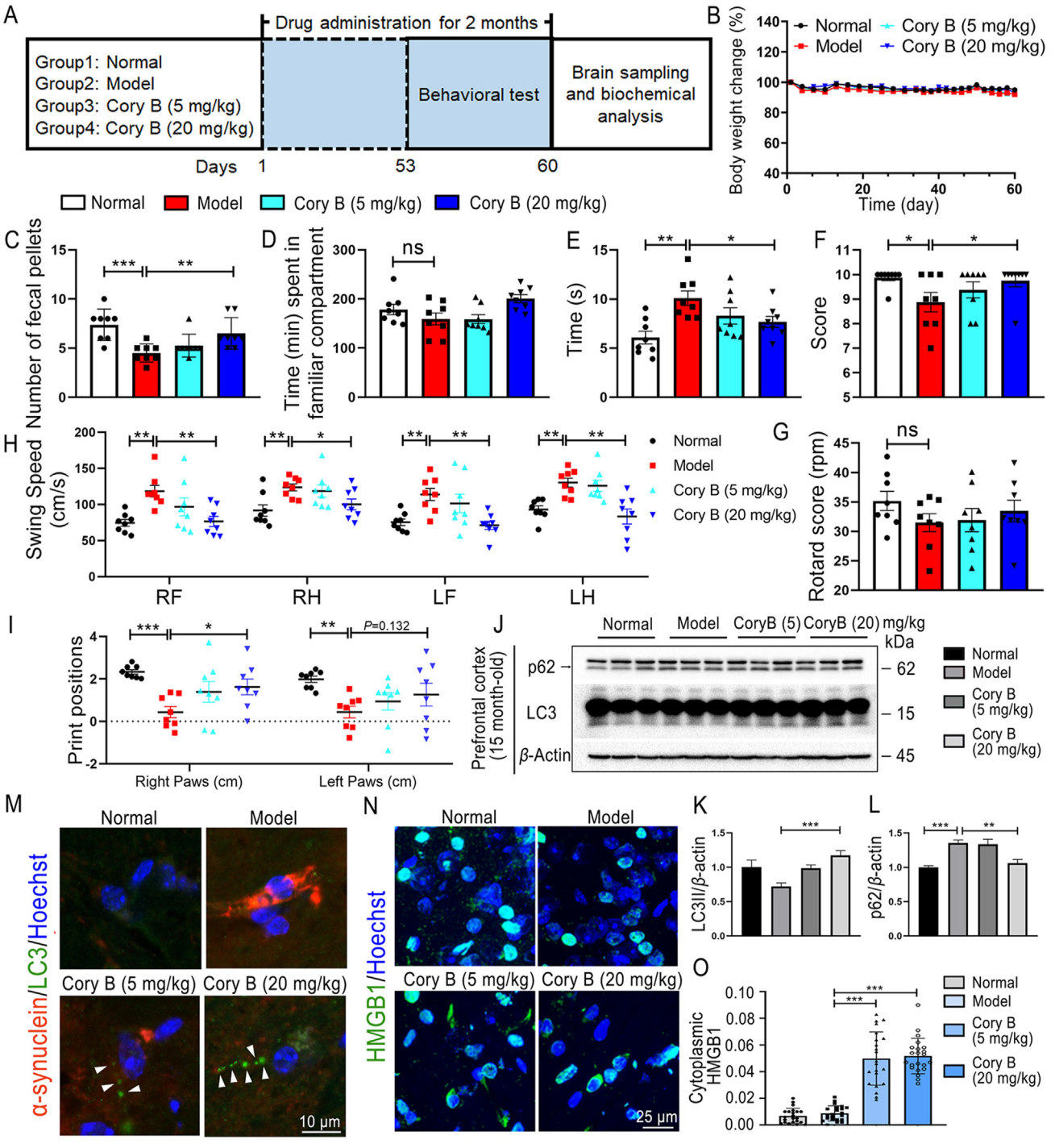

Figure 8 Corynoxine B (Cory B) improved behavioral performance in 15-month-old PD transgenic mice and induced autophagy *in vivo*. (A) Protocol of animal experiments. (B) Body weight changes of each group. (C) In constipation test, total fecal pellets produced in 15 min. (D) In olfactory discrimination test, time spent in familiar compartment. (E) In balance beam test, time to traverse beam apparatus. (F) In horizontal bar test, mice's performance was scored based on the time they spent on the rod (G) In rotarod test, the speed at which the mice fell off the apparatus. (H, I) In CatWalk test analysis, quantitative assessment of footfalls and motor performance. Above quantifications are shown as mean ± SEM (*$P < 0.05$; **$P < 0.01$; ***$P < 0.001$; ns, no significance; $n = 8$ mice). (J–L) Prefrontal cortex of 15-month-old mice were extracted with RIPA lysis buffer (Medium) for Western blot analysis. Expression levels of p62 and LC3II were assessed. The quantifications are shown as mean ± SEM(**$P < 0.01$, ***$P < 0.001$, $n = 5$ mice). (M) IF of midbrain staining α-synuclein and LC3. Fluorescence was observed under a confocal microscope, and representative images are shown. Arrows indicate LC3 puncta. (N) IF of midbrain staining HMGB1. Fluorescence was observed under a confocal microscope, and representative images are shown. (O) Quantification of cytoplasmic HMGB1 in two ventral midbrain regions of 3 mice per group. The quantifications are shown as mean ± SEM (**$P < 0.01$, ***$P < 0.001$).

Cory B intervention. Midbrain sections were co-stained with α-syn and LC3, and, as expected, more LC3 puncta formed in the Cory B-treated group (Fig. 8M). These data suggest that Cory B induced autophagy in mice brain. Furthermore, we investigated the effect of Cory B on HMGB1 levels in tissues, and found that Cory B significantly increased the cytoplasmic HMGB1 level in these mouse model samples (Fig. 8N and O), indicating the regulatory role of Cory B on HMGB1 *in vivo*.

4. Discussion

Our preliminary study had found that Cory B induced autophagy in a Beclin 1-dependent manner and efficiently promoted α-syn degradation in multiple PD cell models. In this article, we proved that Cory B activates PI3KC3 activity/autophagy by directly binding to HMGB1/2 and that Cory B exerts neuroprotective effects in α-syn over-expression fly and rodent PD models by promoting α-syn clearance.

Misfolded α-syn is the main component of LBs in the brains of PD patients. A series of missense mutations in the α-syn gene (*SNCA*) including A53T and A30P have been identified as being related to familial PD[27]. In addition, double or triple *SNCA* has been shown to be sufficient for PD initiation, indicating that the α-syn expression level is a key factor in PD development[28,29]. Lowering α-syn levels has been reported to rescue neurodegeneration in multiple α-synucleinopathy PD models[8,9]. α-syn A53T transgenic mice can well simulate histological characterization of α-syn pathology in humans; however, these mice display delayed-onset motor deficits followed by rapid death with huge individual differences[30]. Furthermore, there is no obvious DA neuron loss in these mice (Supporting Information Fig. S4)[25]. Here, we observed α-syn pathology, early non-motor symptoms, and motor behavioral abnormalities in 15-month-old heterozygous mice, and found that behavioral deficits in PD mice were most detectable in the balance beam test. Cory B treatment improved the behavior performance of PD transgenic mice (Fig. 8C–I).

The PI3KC3 complex is a key signaling complex required for autophagy. Our results showed that Cory B has little effect on the mTORC1 and AMPK pathways (Fig. S1), while knockdown of *Becn1* can completely block Cory B-induced autophagy[8,9]. From the effect of Cory B on PC12 and N2a cells, we conclude that there is no significant difference in the expression levels of VPS34 and Atg14 L, while the expression level of Beclin 1 in PC12 and the corresponding autophagy induction were significantly lower than those in N2a cells (Fig. S1). These results suggest a critical role for Beclin 1 in Cory B-induced autophagy induction. Recent studies have shown that cytoplasmic HMGB1 is a novel Beclin 1-binding protein. HMGB1 C106 is important for its translocation between the nucleus and cytoplasm. The C23 and C45 cysteine sites of HMGB1 A-box bind to Beclin 1 through disulfide bonds, thereby promoting the separation of Beclin 1 from Bcl-2 to induce autophagy[5,31]. Although the role of HMGB1 in autophagy induction has been repeatedly reported, there are some contrary reports disputing the involvement of HMGB1 in autophagy[32]. A possible explanation is that cells may have other proteins to compensate for the loss of HMGB1[33]. In this study, we showed that HMGB2, a homolog of HMGB1, is also required for autophagy and acts together with HMGB1 in autophagy induction, thus providing direct evidence that HMGB1 and HMGB2 can substitute for each other to regulate autophagy. Regarding the mechanism by which HMGB2 regulates autophagy, we speculate that HMGB2 and HMGB1 act in similar ways based on their highly similar structures and functions, as well as the existing molecular docking results. The mechanism by which HMGB2 influences autophagy remains to be confirmed, and the effects of HMGB2's C23, C45 and C106 sites on its translocation and protein binding in physiological and autophagic states remain to be verified.

Dopamine replacement therapies are currently the most common and effective approach for the treatment of PD, although they cannot prevent the disease development and they have unavoidable long-term side effects[34]. Hunting for new drugs with disease-modifying properties is an urgent task. Autophagy enhancement has been regarded as a therapeutic strategy against PD; however, autophagy inducers showing anti-PD properties in animal PD models are still rare[4]. Here, we demonstrate that Cory B, a natural alkaloid, can induce autophagy and promote the clearance of α-syn in fly and rodent models of PD (Figs. 6 and 7), highlighting its potential as a candidate disease-modifying drug for PD therapy.

An increasing number of autophagy inducers have been reported in recent years[23]; however, drugs targeting mTOR-independent autophagy inducers are rarely identified. The lack of knowledge about the targets of autophagy inducers limits the understanding of novel mechanisms of autophagy regulation and the further optimization of structures of compounds based on target information. In this study, we showed that Cory B directly binds to HMGB1/2 and promotes Beclin 1/VPS34 complex activity for autophagy induction. The docking results showed that Cory B binds to a cavity near HMGB1/2 C106 and that this site is important for the nuclear localization of HMGB1/2. Further structural characterization of the binding pattern between Cory B and HMGB1/2 will help to elucidate the mechanism of Cory B action and provide precise information for the structural optimization of Cory B.

5. Conclusions

This study reveals that Cory B regulates PI3KC3 activity/autophagy by binding to HMGB1/2, and establishes that Cory B exerts neuroprotective effects against PD development *in vivo* by promoting α-syn clearance.

Acknowledgments

This study was supported by the National Natural Science Foundation of China (No. 82271455), the Guangdong Basic and Applied Basic Research Foundation (No. 2022A1515012416, China), the Science and Technology Development Fund, Macau SAR (No. 0128/2019/A3, China), the Shenzhen Fundamental Research Program (No. SGDX20210823103804030, China) and the University of Macau grants (No. MYRG2022-00094-ICMS, China) awarded to Jia-hong Lu. The study also partly supported by Hong Kong Health and Medical Research Fund (HMRF/17182551, HMRF/09203776, China) and the Hong Kong General Research Fund (HKBU 12100618, HKBU 12101022, China) from Hong Kong Government and the Research Fund from Hong Kong Baptist University (HKBU/RC-IRCs/17-18/03, IRCMS/19-20/H02, China) awarded to Min Li.

Author contributions

Conceptualization: Min Li and Jiahong Lu; Methodology: Qi Zhu, Juxian Song and Jiahong Lu; Investigation:Qi Zhu, Juxian Song,

Jiayue Chen, Zhenwei Yuan, Liangfeng Liu, Liming Xie, Qiwen Liao and Xiu Chen; Formal Analysis: Jiayue Chen, Yepiao Yan Richard D. Ye, Jieqiong Tan and Chris Soon Heng Tan; Manuscript-Original Draft: Qi Zhu; Resources, Min Li and Jiahong Lu; Writing-Review & Editing: Juxian Song, Min Li and Jiahong Lu; Supervision: Min Li and Jiahong Lu.

Conflicts of interest

The authors declare no conflicts of interest.

Appendix A. Supporting information

Supporting data to this article can be found online at https://doi.org/10.1016/j.apsb.2023.03.011.

References

1. Uversky VN. α-Synuclein misfolding and neurodegenerative diseases. *Curr Protein Pept Sci* 2008;**9**:507−40.
2. Deng Z, Dong Y, Zhou X, Lu JH, Yue Z. Pharmacological modulation of autophagy for Alzheimer's disease therapy: opportunities and obstacles. *Acta Pharm Sin B* 2022;**12**:1688−706.
3. Wu MY, Wang EJ, Feng D, Li M, Ye RD, Lu JH. Pharmacological insights into autophagy modulation in autoimmune diseases. *Acta Pharm Sin B* 2021;**11**:3364−78.
4. Zhang K, et al. Targeting autophagy using small-molecule compounds to improve potential therapy of Parkinson's disease. *Acta Pharm Sin B* 2021;**11**:3015−34.
5. Tang D, et al. Endogenous HMGB1 regulates autophagy. *J Cell Biol* 2010;**190**:881−92.
6. Lu J, et al. NRBF2 regulates autophagy and prevents liver injury by modulating Atg14L-linked phosphatidylinositol-3 kinase III activity. *Nat Commun* 2014;**5**:3920.
7. Zhou J, Zhou S. Antihypertensive and neuroprotective activities of rhynchophylline: the role of rhynchophylline in neurotransmission and ion channel activity. *J Ethnopharmacol* 2010;**132**:15−27.
8. Lu JH, et al. Isorhynchophylline, a natural alkaloid, promotes the degradation of α-synuclein in neuronal cells *via* inducing autophagy. *Autophagy* 2012;**8**:98−108.
9. Lu JH, et al. Isorhynchophylline, a natural alkaloid, promotes the degradation of α-synuclein in neuronal cells *via* inducing autophagy. *Autophagy* 2012;**8**:864−6.
10. Chesselet MF, Richter F, Zhu C, Magen I, Watson MB, Subramaniam SR. A progressive mouse model of Parkinson's disease: the Thy1-αSyn ("Line 61") mice. *Neurotherapeutics* 2012;**9**:297−314.
11. Sampson TR, et al. Gut microbiota regulate motor deficits and neuroinflammation in a model of Parkinson's disease. *Cell* 2016;**167**:1469. 80.e12.
12. Rial D, et al. Behavioral phenotyping of Parkin-deficient mice: looking for early preclinical features of Parkinson's disease. *PLoS One* 2014;**9**:e114216.
13. Brooks SP, Dunnett SB. Tests to assess motor phenotype in mice: a user's guide. *Nat Rev Neurosci* 2009;**10**:519−29.
14. Luong TN, Carlisle HJ, Southwell A, Patterson PH. Assessment of motor balance and coordination in mice using the balance beam. *J Vis Exp* 2011:e2376.
15. Deacon RM. Measuring motor coordination in mice. *J Vis Exp* 2013:e2609.
16. Garrick JM, Costa LG, Cole TB, Marsillach J. Evaluating gait and locomotion in rodents with the CatWalk. *Curr Protoc* 2021;**1**:e220.
17. Pitzer C, Kurpiers B, Eltokhi A. Gait performance of adolescent mice assessed by the CatWalk XT depends on age, strain and sex and correlates with speed and body weight. *Sci Rep* 2021;**11**:21372.
18. Zhu Q, et al. Lycorine, a natural alkaloid, promotes the degradation of α-synuclein *via* PKA-mediated UPS activation in transgenic Parkinson's disease models. *Phytomedicine* 2021;**87**:153578.
19. Klucken J, et al. Clinical and biochemical correlates of insoluble α-synuclein in dementia with Lewy bodies. *Acta Neuropathol* 2006;**111**:101−8.
20. Wu MY, et al. PI3KC3 complex subunit NRBF2 is required for apoptotic cell clearance to restrict intestinal inflammation. *Autophagy* 2021;**17**:1096−111.
21. Hashimoto M, Girardi E, Eichner R, Superti-Furga G. Detection of chemical engagement of solute carrier proteins by a cellular thermal shift assay. *Acs Chem Biol* 2018;**13**:1480−6.
22. Sanjana NE, Shalem O, Zhang F. Improved vectors and genome-wide libraries for CRISPR screening. *Nat Methods* 2014;**11**:783−4.
23. Dong Y, et al. Autophagy modulator scoring system: a user-friendly tool for quantitative analysis of methodological integrity of chemical autophagy modulator studies. *Autophagy* 2020;**16**:195−202.
24. Martinez Molina D, et al. Monitoring drug target engagement in cells and tissues using the cellular thermal shift assay. *Science* 2013;**341**:84−7.
25. Ke M, et al. Comprehensive perspectives on experimental models for Parkinson's disease. *Aging Dis* 2021;**12**:223−46.
26. Poirier AA, Aube B, Cote M, Morin N, Di Paolo T, Soulet D. Gastrointestinal dysfunctions in Parkinson's disease: symptoms and treatments. *Parkinsons Dis* 2016;**2016**:6762528.
27. Flagmeier P, et al. Mutations associated with familial Parkinson's disease alter the initiation and amplification steps of α-synuclein aggregation. *Proc Natl Acad Sci U S A* 2016;**113**:10328−33.
28. Singleton AB, et al. α-Synuclein locus triplication causes Parkinson's disease. *Science* 2003;**302**:841.
29. Ahn TB, et al. α-Synuclein gene duplication is present in sporadic Parkinson disease. *Neurology* 2008;**70**:43−9.
30. Giasson BI, Duda JE, Quinn SM, Zhang B, Trojanowski JQ, Lee VM. Neuronal α-synucleinopathy with severe movement disorder in mice expressing A53T human α-synuclein. *Neuron* 2002;**34**:521−33.
31. Kang R, Zeh HJ, Lotze MT, Tang D. The Beclin 1 network regulates autophagy and apoptosis. *Cell Death Differ* 2011;**18**:571−80.
32. Huebener P, et al. High-mobility group box 1 is dispensable for autophagy, mitochondrial quality control, and organ function *in vivo*. *Cell Metab* 2014;**19**:539−47.
33. Zhu X, et al. Cytosolic HMGB1 controls the cellular autophagy/apoptosis checkpoint during inflammation. *J Clin Invest* 2015;**125**:1098−110.
34. De Deurwaerdere P, Di Giovanni G, Millan MJ. Expanding the repertoire of L-DOPA's actions: a comprehensive review of its functional neurochemistry. *Prog Neurobiol* 2017;**151**:57−100.